RSC Advances

PAPER

View Article Online
View Journal | View Issue

Check for updates

Cite this: *RSC Adv.*, 2022, **12**, 27431

Surface state modulation of blue-emitting carbon dots with high quantum yield and high product yield†

Mingxiu Lei,[a] Yanting Xie,[a] Lin Chen,[ab] Xinghua Liu,[a] Yongzhen Yang,[*ab] Jingxia Zheng*[ab] and Qiang Li*[c]

Received 6th September 2022
Accepted 16th September 2022

DOI: 10.1039/d2ra05623b

rsc.li/rsc-advances

In order to explore the surface state modulation mechanism of carbon dots (CDs) with high quantum yield (QY) and high product yield (PY), CDs were synthesized from different carbon sources with different contents of oxygen-containing functional groups and different silane coupling agents with nitrogen-containing functional groups. The highest QY of as-prepared CDs can reach 97.32% and the PY values of CDs are all high ranging from 46.33–58.76%. It is found that the high content of C=O and pyrrolic N on the surface of CDs can endow CDs with high QY. Moreover, the PY of CDs not only depends on whether CDs have the crosslinked structure, but also is closely and positively correlated with pyridinic N. Consequently, our findings suggest that raw materials rich in carboxyl groups and amino groups are beneficial to the synthesis of CDs with high QY, and whether CDs with crosslinked structure and high content of pyridinic N decide the high PY of CDs. This work provides a theoretical guidance for large-scale synthesis of CDs with high QY and high PY.

Introduction

As recently emerging fluorescent materials, carbon dots (CDs) are attracting increasing attention in many fields, including bio-imaging, photocatalysis, fluorescent sensors, drug delivery, solar cells, visible light communication and light-emitting diodes (LEDs),[1–13] due to their superior photoluminescence, good photostability, low toxicity, excellent biocompatibility, low cost and readily available raw materials.[7,9,14] Fluorescent quantum yield (QY) and product yield (PY) of CDs are two important attributes to judge whether CDs can act as efficient luminous materials for their practical applications.[15] Therefore, the synthesis of fluorescent CDs with both high PY and high QY are greatly desired.

A host of works to improve the fluorescent QY and PY of CDs have been reported and their related mechanisms also have been investigated.[1,15–18] The studies showed that the QY and PY of CDs can be modulated through controlling the surface states of CDs with different functional groups from raw materials.[19] Sun *et al.* demonstrated that N-doping with amino compounds can greatly improve the QY of N-doped blue-emitting CDs up to 94%.[16] Zhang *et al.* synthesized a series of blue-emitting CDs with high QYs of 99% using amino compounds containing hydroxyl groups, which can easily provide N-doping and strong electron-donating hydroxyl, suggesting that the synergy between the hydroxyl and graphitic nitrogen can give rise to a much-improved radiative transition rate and ultra-high QY.[15] Wu *et al.* prepared blue-emitting CDs from yeast extract powder including peptides, amino acids, minerals, and B-complex vitamins with abundant oxygen-containing (O-containing) functional groups by a one-step hydrothermal method at large scale, and the PY of CDs reaches up to 65.8%.[17] Zhu *et al.* developed a rapid and facile magnetic hyperthermal (MHT) method for preparing blue-emitting Zn-CDs with QY of 55% and PY of 69% on a large scale and speculated that the enhanced production efficiency of CDs results from the intensified energy transfer of the MHT reaction process, with respect to conventional methods.[14] In our previous work,[20] nitrogen and silicon co-doped blue fluorescent CDs (b-CDs) with high QY of 97.32% and high PY of 52.56% for white light-emitting diodes (LEDs) were reported. Citric acid with abundant O-containing functional groups and *N*-[3-(trimethoxysilyl)propyl]ethylenediamine (KH-792) as the nitrogen dopant increase the electron cloud density on the surface of b-CDs, and thus promote the high QY of b-CDs.[20] KH-792 with large spatial stereoscopic structure is beneficial to the improved structural stability of b-CDs, which further ensures the b-CDs with high PY.[20] This work indicated that surface state played a key role in the obtainment of high QY and PY. Despite the great developments in this area, the surface state regulation mechanism of CDs with both high QY and high PY has been rarely reported.

[a]*Key Laboratory of Interface Science and Engineering in Advanced Materials, Ministry of Education, Taiyuan University of Technology, Taiyuan 030024, China. E-mail: yyztyut@126.com; zhengjingxia@tyut.edu.cn*

[b]*Shanxi-Zheda Institute of Advanced Materials and Chemical Engineering, Taiyuan 030032, China*

[c]*Intervention Department of the Second Hospital of Shanxi Medical University, Taiyuan 030001, China. E-mail: liqiang8702226@163.com*

† Electronic supplementary information (ESI) available. See https://doi.org/10.1039/d2ra05623b

Open Access Article. Published on 27 September 2022. Downloaded on 2/14/2026 12:02:08 AM.
This article is licensed under a Creative Commons Attribution-NonCommercial 3.0 Unported Licence.

Open Access Article. Published on 27 September 2022. Downloaded on 2/14/2026 12:02:08 AM.
This article is licensed under a Creative Commons Attribution-NonCommercial 3.0 Unported Licence.

Therefore, the surface state regulation strategy for preparing CDs with high QY and high PY is essential for their future widespread utilization. It is well known that different functional groups can form various surface states during the formation of CDs, and raw materials dominate the surface structure of CDs, thus affecting the QY and PY of CDs. Therefore, it is necessary to clarify the effects of surface states on QY and PY of CDs.

Hence, the different carbon sources and silane coupling agents, with different contents of O-containing and nitrogen-containing (N-containing) functional groups, were selected to synthesize a series of blue fluorescent CDs by a hydrothermal method. On this basis, by characterizing QY, PY, the structure, composition and optical properties of as-prepared CDs, the internal relationship between the structure of raw material and QY and PY of CDs is revealed, and the surface state modulation mechanism of CDs with high QY and high PY is proposed in an attempt to provide theoretical guidance for synthesizing CDs with high QY and high PY. It was found that the QY and PY of CDs are closely related to O- and N-containing functional groups from raw materials, such as carboxyl, hydroxyl, methoxy and amino groups. The high QY of CDs is attributed to the high content of C=O and pyrrolic N on their surfaces. The CDs with the excitation independence property and long lifetime generally have high QY. The crosslinking structure is responsible for the high PY of the CDs, and pyridinic N can enhance the PY of CDs while amino N can weaken the PY of the CDs.

Experimental section

Materials and methods

The raw materials, including citric acid monohydrate (CA), anhydrous citric acid (a-CA), anhydrous oxalic acid (OA), lactic acid (LA), malic acid (MA), tartaric acid (TA), *N*-[3-(trimethoxysilyl)propyl]-ethylenediamine (KH-792), 3-(2-aminoethylamino)propyl-dimethoxymethyl silane (KH-602) and 3-aminopropyltri-methoxy silane (KH-540), were all purchased from Tianjin Guangfu Chemical Reagent Co., Ltd. Quinine sulphate was acquired from Sinopharm Chemical Reagent Co., Ltd. Sulfuric acid was supplied by Luoyang Chemical Reagent Factory. All chemicals were of analytical grade and used without further purification. Deionized water was used throughout this experiment.

Synthetic procedures

First of all, in order to explore the influence of O-containing functional groups on CDs, the dosage of silane coupling agent (KH-792) as precursors was fixed, and then carbon sources with different O-containing functional groups (including TA, MA, LA, OA, a-CA and CA) were chosen to synthesize different CDs (including TA-, MA-, LA-, OA-, a- and CA-CDs) by hydrothermal method. For the synthesis of CA-CDs, CA (1.0507 g), KH-792 (21.8 mL) and deionized water (40 mL), in turn, were added into a 100 mL Teflon lined stainless steel autoclave, and heated at 200 °C for 6 hours. After cooling to room temperature naturally, the solution, which appeared from colourless to orange, was filtered using 0.22 μm membrane to remove larger and unreacted impurities. Then it was dialyzed using the dialysis bag (molecular weight cut-off: 1000 Da) for 3 hours. Finally, the resultant solid products were obtained through freeze drying at −80 °C for 48 hours. Synthesis of TA-, MA-, LA-, OA-, and a-CDs followed the procedure for the synthesis of CA-CDs.

Secondly, to investigate synergistic influence of O- and N-containing functional groups on CDs, the mass of carbon sources (CA) was fixed, and silane coupling agents with different O- and N-containing functional groups (including KH-540, KH-602 and KH-792) were selected to synthesize different CDs (including 540-, 602- and CA-CDs) by hydrothermal method. Synthesis of 540- and 602-CDs followed the procedure for the synthesis of CA-CDs.

Characterization

The morphology and microstructure of CDs were obtained by transmission electron microscopy (TEM) and high-resolution transmission electron microscopy (HRTEM) on a JEOL JEM-2010 using an accelerating voltage of 200 kV. Raman spectra were measured with HORIBA Scientific LabRAM HR Evolution (785 nm laser). Fourier transform infrared (FTIR) analysis of CDs was carried out in the form of KBr pellets with a BRUKER TENSOR 27 spectrometer. The elemental analysis (EA) of CDs was conducted on an ELEMENTAR Vario EL/micro cube. The X-ray photoelectron spectroscopy (XPS) spectra of samples were recorded on a Kratos AXIS ULTRA DLD X-ray photoelectron spectrometer with an exciting source of Al Kα = 1486.6 eV. UV-visible (UV-vis) absorption analysis was obtained using a Hitachi U3900 UV-vis spectrophotometer. The photoluminescence (PL) spectra were recorded using a Horiba Fluoromax-4 luminescence spectrometer equipped with a Xe lamp as excitation source. The fluorescence decay status and fluorescence lifetime of CDs were measured by an Edinburgh F980 Transient Fluorescence & Phosphorescence spectrometer.

QY measurements

QY of CDs was determined by a relative method[21] and measured by using quinine sulphate (QY = 54 ± 0%) in 0.1 M sulfuric acid solution as standard. The QY of CDs (in water) was calculated according to eqn (1):

$$Q = Q_s(A_s/A_x)(G_x/G_s)(n_x/n_s)^2 \quad (1)$$

where Q is QY, A is optical density, G is measured integrated emission intensity, and n is the refractive index of solvent. In the solutions of this study, $n_x/n_s = 1$. The subscripts s and x refer to the standard quinine sulphate and the testing sample, respectively. In order to minimize re-absorption effects, the concentration of CDs and quinine sulphate for estimation should be selected to adjust the optical absorbance values below 0.1 at 360 nm.

PY measurements

The PY value of CDs was determined according to eqn (2):

$$PY = [m_{CDs}/(m_c + m_s)] \times 100\% \quad (2)$$

© 2022 The Author(s). Published by the Royal Society of Chemistry

Open Access Article. Published on 27 September 2022. Downloaded on 2/14/2026 12:02:08 AM.
This article is licensed under a Creative Commons Attribution-NonCommercial 3.0 Unported Licence.

where m_{CDs}, mc and m_s refer to the mass of as-prepared CD powder, carbon source and silane coupling agent, respectively.

Results and discussion

Influence of O-containing functional groups on CDs

Table S1† shows the molecular structures of carbon sources, and the QY and PY values of CDs synthesized with different carbon sources. The relationship between O-containing functional groups of carbon source and QY and PY of CDs was intuitively analysed: the QY of CDs was obviously different, which may be because of the difference in the content and types of the O-containing functional groups (including carboxyl, hydroxyl groups, and water molecule) of carbon sources. At the same time, the PY of CDs, ranging in 52.56–58.76%, were high and similar, which may be attributed to the crosslinking structure of CDs.[22,23] It demonstrates that the degree of crosslinking reaction between different carbon sources and silane coupling agents may be similar.

Thus, it can be seen that the QY of CDs synthesized with different carbon sources is closely related to the content of carboxyl and hydroxyl groups, and the PY values of CDs depend on whether the reactants can undergo crosslink reaction to obtain CDs with the crosslinking structure. To further explore this mechanism, the morphology, structure and optical properties of different CDs were characterized and compared as follow.

Morphology and structure characterizations. TEM and HRTEM images in Fig. 1a–f reveal that CDs synthesized with different carbon sources are all spherical in shape and

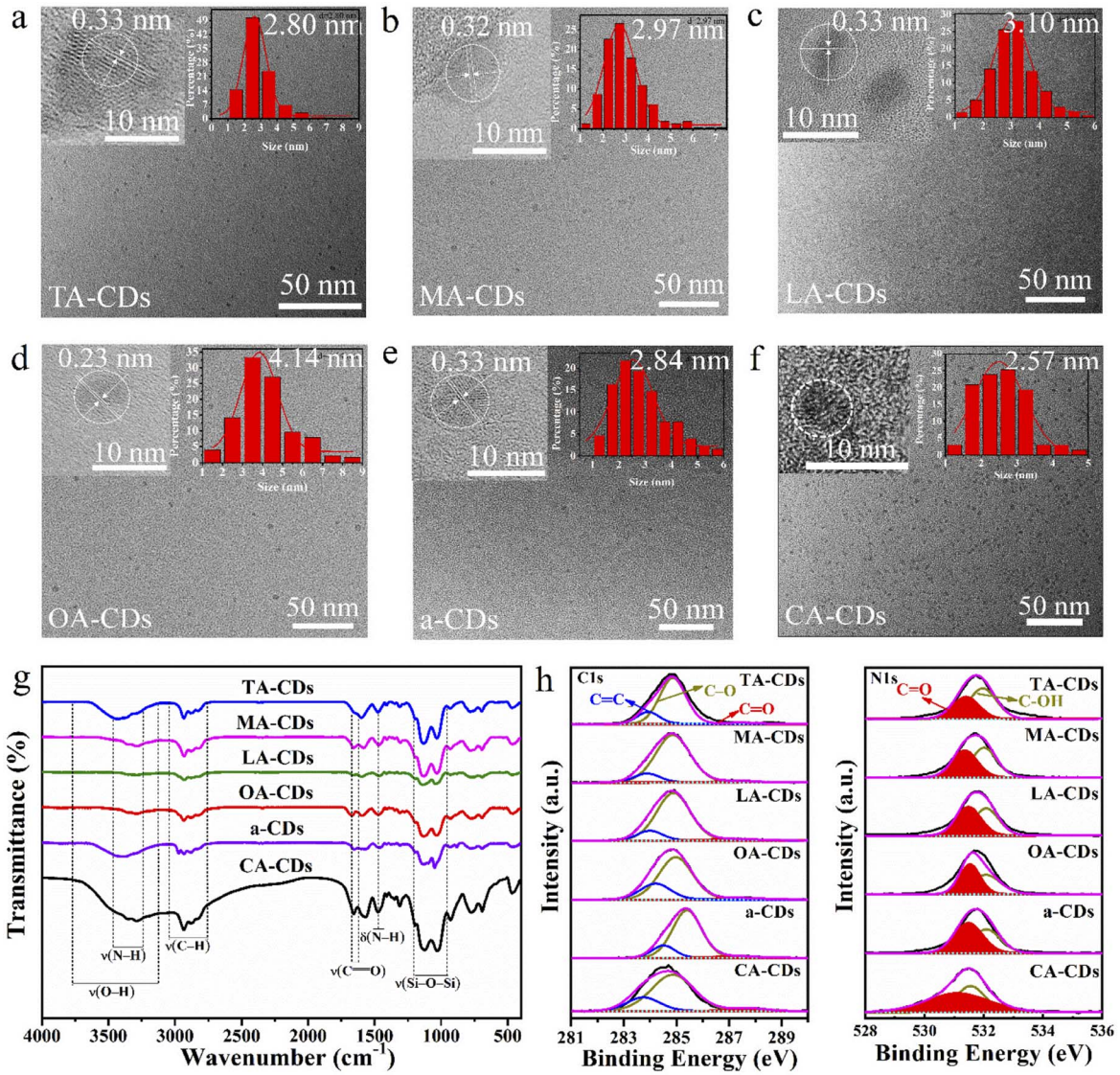

Fig. 1 TEM images of CDs synthesized with different carbon sources: (a) TA-CDs, (b) MA-CDs, (c) LA-CDs, (d) OA-CDs, (e) a-CDs and (f) CA-CDs, silane coupling agent is KH-792. Inset: HRTEM images and the corresponding size distribution histograms of CDs. (g) FTIR spectroscopy of CDs synthesized with different carbon sources (silane coupling agent is KH-792). (h) XPS spectrum of CDs synthesized with different carbon sources (silane coupling agent is KH-792).

Open Access Article. Published on 27 September 2022. Downloaded on 2/14/2026 12:02:08 AM. This article is licensed under a Creative Commons Attribution-NonCommercial 3.0 Unported Licence.

uniformly dispersed, with the particle size ranging from 2.57 to 4.14 nm. The size distribution of CDs is consistent with the Gaussian distribution and CDs except CA-CDs all have obvious lattice fringe. The interplanar crystal spacings of TA-, LA-, and a-CDs are all about 0.33 nm, close to the (002) crystal face of graphite.[24] The interplanar crystal spacings of MA-CDs is 0.32 nm, corresponding to the (002) of graphite. The interplanar crystal spacings of OA-CDs is 0.23 nm, corresponding to the (100) of graphite.[25] CA-CDs are amorphous structure without obvious lattice fringe. LA-CDs have mixed crystalline and amorphous structure. The different crystal plane spacings of the CDs from different carbon sources declare their different crystal structures. Besides, compared with TA-, MA-, LA-, OA- and a-CDs, CA-CDs are more uniform in size distribution. The change trend of particle sizes of CDs is not consistent with that of QY and PY of CDs. With the increase of the average particle size of CA-, TA-, a-, MA-, LA- and OA-CDs, the corresponding QY value is first decreasing, then increasing and lastly decreasing, and meanwhile the corresponding PY value is little changed. Therefore, it can be speculated that the difference in QY and PY of CDs from different carbon sources should not originate from the quantum size effect.[19,26,27] Meanwhile, the Raman spectra in the Fig. S1† reveals that these CDs possess a certain degree of graphitization. The disordered D band at around 1310 cm^{-1} and crystalline G band at around 1460 cm^{-1} in the Raman spectra, indicating the coexistence of disordered carbon and graphitic carbon structures in the six types of CDs.[28] The larger intensity ratio I_G/I_D means the higher graphitization degree. With the increasing I_G/I_D value of MA-CDs, LA-CDs, a-CDs, TA-CDs, CA-CDs and OA-CDs, the corresponding QY value changes irregularly, and the PY value does not change significantly. Therefore, the graphitization degree of carbon core state is not a key factor affecting QY and PY of CDs from different carbon sources.

The surface functional groups of CDs from different carbon sources were characterized by FTIR spectroscopy. The results (Fig. 1g) show that the organosilane functionalization and formation of amide groups on the six types of CDs surface can be confirmed by the typical bands at 1030 and 1124 cm^{-1} originating from the stretching vibration of Si–O–Si, and at 1657 cm^{-1} arising from the –CONH– bond, which proves that carboxyl groups and hydroxyl groups in different carbon sources have undergone dehydration, condensation and crosslinking reactions with amino groups and siloxane groups in silane coupling agents.[20,29] The vibration of the C=O bond from the carboxyl group is also found on the surface of CDs at 1660 cm^{-1}. The intensity of O–H and C=O peak (relative to that of –CONH–) of CA-CDs with the highest QY is the highest, indicating that compared to other carbon sources, CA reacting with KH-792 has the highest degree of hydrolysis and form more amide bonds. Meanwhile, it proves that the QY of CA-CDs is higher than that of a-CDs is because the water molecules in the CA intensify the hydrolysis degree of KH-792 and the degree of reaction with CA.

As shown in Table S2,† the element analysis of CDs indicates all CDs from different carbon sources contain C, H, N, O and Si elements. CA-CDs has the highest QY and the highest surface oxygen content, manifesting the high content of oxygen of carbon source may contribute to the high QY of CA-CDs.[15] For the full-scan XPS spectra of CDs as shown in Fig. S2,† the strong peaks of C 1s and O 1s indicate that all CDs are mainly composed of C and O elements, while relatively weak peaks of N 1s, Si 2p and Si 2s demonstrate that KH-792 involves in the formation of CDs, which introduces new surface states such as N-containing functional groups. This is consistent with the results of FTIR and element analysis. The analysis results of XPS for CDs from different carbon sources are shown in Table S3.† The element content of XPS is the percentage of element atoms on the surface of CDs. Element analysis of CDs is the mass percentage of their overall element. The change trend of the element analysis results of XPS is consistent with that of element analysis.

To in-depth analyse the relationship between the QY of CDs from different carbon sources and their surface structures, the C 1s and O 1s spectra of CDs in Fig. 1h were recorded, and the amounts of different types of chemical bonds in CDs were carried on the quantitative analysis, as shown in Table 1. The C 1s spectrum can be divided into three peaks (C=C, C–C and C=O), and the O 1s spectrum can be deconvoluted into C=O and C–OH. The increasing percentage of C=C on the surface of MA-CDs, LA-CDs, a-CDs, TA-CDs, CA-CDs and OA-CDs is consistent with the Raman results. With the increased QY values of CDs, both the peak intensity and percentage composition of C=O on the surface of CDs have obvious increased in Fig. 1h and Table 1. Thus, it can be suggested that the content of C=O bond and the QY of CDs have an obvious and distinct relationship. Therefore, with the gradually increase of the content of C=O bond, the oxidation degree on the surface of CDs enhances gradually, their surface defect sites increase, and then the corresponding exciton capture centre increases, and accordingly, the QY of CDs will rise.[30]

Optical properties. Fig. S3† shows the UV-vis absorption spectra of CDs from different carbon sources. CA-CDs and a-CDs show the characteristic absorption bands at 243 nm, which are assigned to the π–π* transition of the aromatic C=C bonds, respectively.[19] CDs all exhibit the absorption peaks centred at 320–360 nm attributed to the n–π* transition of C=O bonds.[31] CA-CDs and a-CDs have high QY values, and their corresponding UV-vis absorption peaks at 360 nm are strong, which qualitatively indicates that the contents of C=O are high.[31] The other four CDs with low QY exhibit weak and similar

Table 1 The amounts of various chemical bonds of CDs synthesized with different carbon sources in XPS spectra (silane coupling agent is KH-792)

	C 1s			O 1s	
CDs	C=C/%	C–C/%	C=O/%	C=O/%	C–OH/%
TA-CDs	18.07	79.82	2.11	40.85	59.15
MA-CDs	12.25	84.82	2.93	47.67	52.33
LA-CDs	13.23	83.02	3.75	51.36	48.64
OA-CDs	24.49	71.84	3.68	52.02	47.98
a-CDs	16.55	79.61	3.84	56.22	43.78
CA-CDs	20.50	73.71	5.79	61.24	38.76

© 2022 The Author(s). Published by the Royal Society of Chemistry

Open Access Article. Published on 27 September 2022. Downloaded on 2/14/2026 12:02:08 AM.
This article is licensed under a Creative Commons Attribution-NonCommercial 3.0 Unported Licence.

absorption peak at around 325 nm. This is consistent with the analysis results of XPS, further confirming that the high content of C=O could promote the synthesis of CDs with high QY. These absorption changes disclose that the surface states of CDs have been changed through changing the contents of O-containing precursors, which significantly affects the photoluminescence performance of CDs.[29]

As an important optical property of CDs, the fluorescence emission spectra of CDs from different carbon sources under various excitation wavelengths are shown in Fig. 2a–f. By comparison, it can be seen that TA-, MA-, LA- and OA-CDs with low QY have a similar feature of excitation-wavelength dependence. The excitation-wavelength dependence may be derived from the heterogeneous size of TA-, MA-, LA- and OA- or diverse surface states.[15] Meanwhile, CA-CDs and a-CDs with high QY have the property of excitation-wavelength independence, which reflects that the surface states of CA-CDs and a-CDs are originated from a single energy level, and almost all of excited electrons can return to the ground state through the radiation route. Therefore, the passivation degree of the trap on the surface of CA-CDs and a-CDs is enhanced, leading to the increase of the fluorescence QY of CA-CDs and a-CDs.[32]

In order to further analyse the fluorescence properties and their origins of CDs from different carbon sources, the fluorescence lifetimes of CDs were measured. The PL decay curves of CDs except a-CDs fit with a double-exponential function and provide PL lifetimes in the range of 9.46–14.62 ns. The PL decay curve of a-CDs fits with a single-exponential function and their lifetime is 18.00 ns (Fig. 2g). The corresponding fitting parameters are as shown in Table S4.† α_1 refers to the proportion of short lifetime τ_1 deriving from carbon nuclear state, and α_2 refers to the proportion of long lifetime τ_2 deriving from surface state. Therefore, the QY of CDs mainly benefits from the contribution of surface states. Fig. 2g illustrates that from top to bottom, the QY of CDs gradually increases, and in the meantime the decay rate of τ is gradually slows down. As a whole, with the increase of the QY values of CDs, the values of long lifetime τ_2 gradually increased, and fluorescence lifetime showed a trend of gradual increase (Table S4†). The increase of fluorescence lifetime may be attributed to the decrease of the non-radiation traps or the increase of emission sites resulting from surface passivation of CDs.[33] Meanwhile, the change trend of lifetime of CDs is consistent with that of the content of C=O bond, which shows the O-containing functional groups on the surface of CDs have great contribution to the QY.

Influence mechanism. Taking into account of all above-mentioned factors, the possible structures of the six kinds of CDs are given in Fig. 3. Carbon sources have different amount of carboxyl and hydroxyl groups. Both carboxyl and hydroxyl groups in carbon sources can undergo dehydration, condensation and crosslinking reactions with amino and methoxy groups in silane coupling agents in the hydrothermal process. For the QY of CDs from different carbon sources, when silane coupling agent (KH-792) remains constant, more O-containing functional groups in carbon source is beneficial to prepare the corresponding CDs with higher QY. On one hand, this is because that the O-containing functional groups especially carboxyl groups of CA can react with the amino group of the silane coupling agent to form an amide bond, which boosts the high QY of CDs; on the other hand, the attached organosilane functional groups on the CD surface could not only serve as surface passivation agents to trap surface electrons, but also as electron donors to increase the electron cloud density, which increases together the probability of electron–hole radiative recombination thus to improve the QY.[33,34] When the number of hydroxyl groups in the carbon source is the same (MA, LA, a-CA and CA), the more carboxyl groups, the higher QY of corresponding as-synthesized CDs. Among them, CA has one more water molecule than a-CA, and the QY of CA-CDs is more 30% higher than a-CDs, which should be because the water molecules contained in CA are conducive to the hydrolysis of KH-792 and promote the reaction. When the number of carboxyl groups in the carbon source is the same (TA, MA and OA), the less the number of hydroxyl groups, the higher the QY of corresponding CDs. It is speculated that hydroxyl groups can condensate and cross-link with silanols groups formed after hydrolysis to form

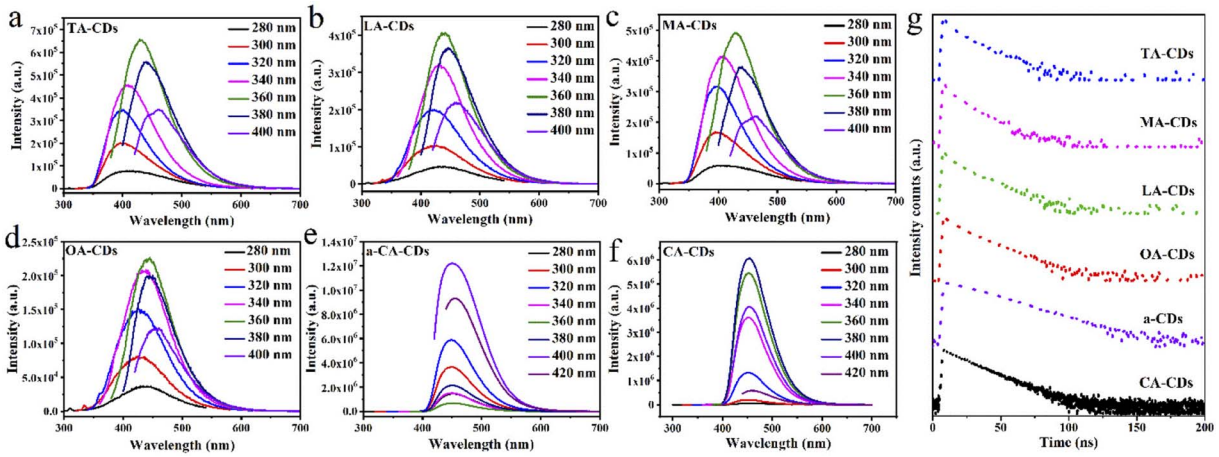

Fig. 2 (a–f) Fluorescence emission spectra and (g) fluorescence decay curve of CDs solutions synthesized with different carbon sources under various excitation wavelengths (silane coupling agent is KH-792).

Open Access Article. Published on 27 September 2022. Downloaded on 2/14/2026 12:02:08 AM.
This article is licensed under a Creative Commons Attribution-NonCommercial 3.0 Unported Licence.

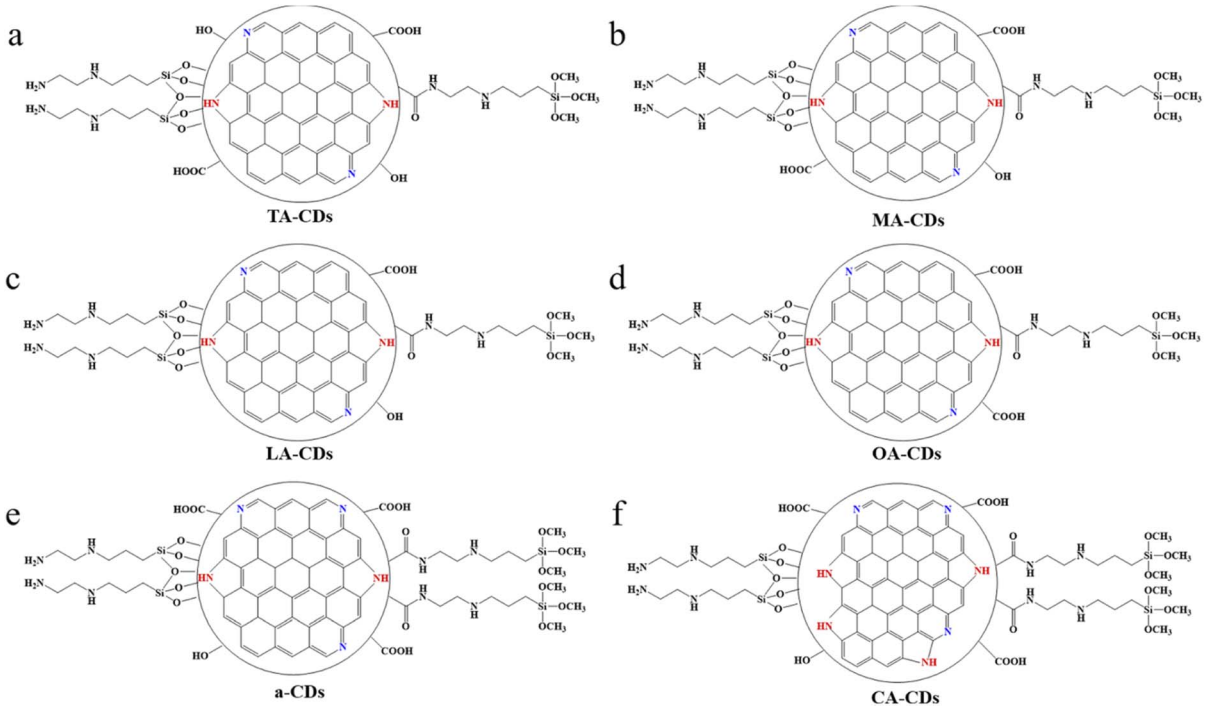

Fig. 3 Schematic structure of CDs synthesized with different carbon sources: (a) TA-CDs, (b) MA-CDs, (c) LA-CDs, (d) OA-CDs, (e) a-CDs and (f) CA-CDs, silane coupling agent is KH-792.

a cross-linked structure with a certain steric hindrance, which obstructs the reaction between carboxyl group and amino group.[35] Generally, CDs with the property of excitation independence and long lifetime have high QY.

Moreover, the PY values of CDs from different carbon sources were high and similar, from 52.56% to 58.76%, this is because the carboxyl and hydroxyl groups from carbon sources and amine and siloxane groups from KH-792 can undergo dehydration, condensation and crosslinking reactions, and the crosslinking structure benefits for the high PY of CDs,[22,23] and the degree of cross-linking reaction between different carbon sources and silane coupling agents may be similar.

To sum up, it was found that the fluorescence of CDs from different carbon sources mainly comes from surface state luminescence rather than the quantum size effect. The influence mechanism of O-containing functional groups on CDs is presented, as shown in Fig. 4. The QY values of CDs synthesized using different carbon sources are closely related to the O-containing functional groups on the surface of carbon sources, specifically, the higher the content of C=O, the higher the QY value of CDs. The PY value of CDs depends on whether CDs has the crosslinking structure.

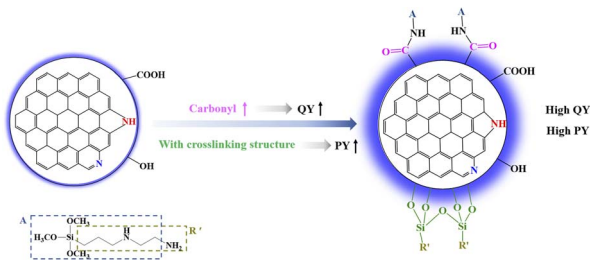

Fig. 4 Schematic of influence mechanism of O-containing functional groups on CDs.

Synergistic influence of O- and N-containing functional groups on CDs

On the basis of the above research, the effects of the introduction of N-containing functional groups on the QY and PY of CDs should be considered, so synergistic influence of O- and N-containing functional groups on CDs was investigated. Table S5† lists the molecular structures of silane coupling agents and the PY and QY values of CDs synthesized with different silane coupling agents. The relationship between O- and N-containing functional groups of silane coupling agent and QY and PY values of CDs is intuitively analysed: silane coupling agents contains different number of methoxy and amino groups, and different chain lengths, so the QY and PY values of corresponding as-synthesized CDs are different. Amino groups and chain length have significant effects on QY of CDs and methoxy group has little influence on QY of CDs. Besides, the PY values of CDs are all high and similar from 46.33% to 58.53%, whose change trend is consistent with that of the PY values of CDs from different carbon sources.

Consequently, it is found that the QY values of CDs synthesized using different silane coupling agents is closely related to the content of amino groups, and the PY values of CDs still depends on whether the reactants can undergo crosslinking reaction. The main text of the article should appear here with headings as appropriate.

© 2022 The Author(s). Published by the Royal Society of Chemistry

Open Access Article. Published on 27 September 2022. Downloaded on 2/14/2026 12:02:08 AM.
This article is licensed under a Creative Commons Attribution-NonCommercial 3.0 Unported Licence.

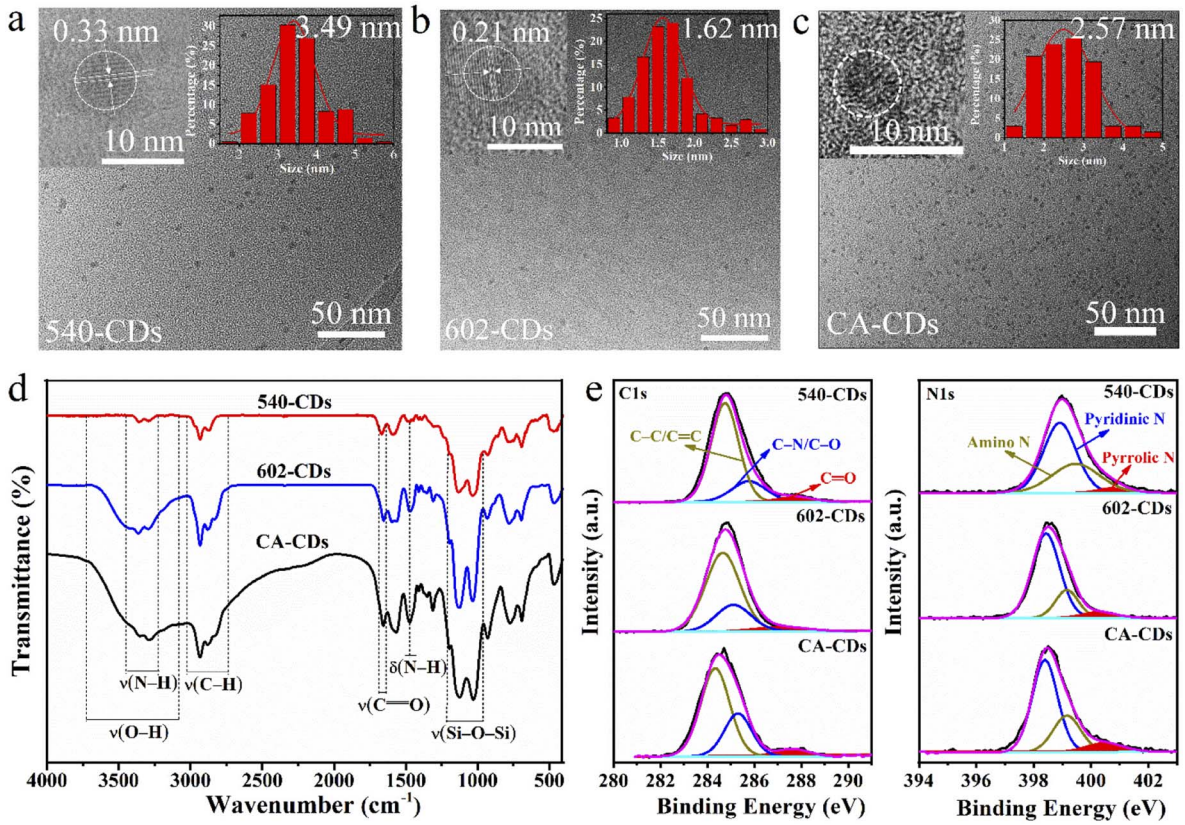

Fig. 5 TEM images of CDs synthesized with different silane coupling agents: (a) 540-CDs, (b) 602-CDs and (c) CA-CDs, carbon source is CA. Inset: HRTEM images and the corresponding size distribution histograms of CDs. (d) FTIR spectroscopy of CDs synthesized with different silane coupling agents (carbon source is CA). (e) XPS spectrum of CDs synthesized with different silane coupling agents (carbon source is CA).

Morphology and chemical structure characterizations. The morphology structures of CDs synthesized with different silane coupling agents are illustrated in Fig. 5a–c. It can be seen that CDs are all spherical and evenly dispersed, and the particle size range is 1.62–3.49 nm. 540- and 602-CDs both have obvious lattice fringe and the lattice spacing are 0.33 and 0.21 nm, which corresponds to the (002) and (100) crystal planes of graphite, respectively.[24,25] CA-CDs are amorphous structure without obvious lattice fringe. These different crystal plane spacings of CDs from different silane coupling agents exhibit their different crystal structures. Besides, compared with 540- and 602-CDs, CA-CDs are more uniform in size distribution. The QY change of CDs has no obvious dependencies with the particle size change of CDs, so the luminescence of CDs synthesized with different silane coupling agents should not originate from the quantum size effect.[26,27] The Raman spectra of these CDs (Fig. S4†) contain a D band at around 1310 cm^{-1} and a G band at around 1460 cm^{-1}, which correspond to the vibration of sp^3 and sp^2 carbon atoms, respectively.[28] However, the QY and PY value of these CDs do not have a significant dependence with the increasing intensity ratio I_G/I_D of 602-CDs, 540-CDs, and CA-CDs. Therefore, the graphitization degree of carbon core state has little effect on the QY and PY of CDs synthesized with different silane coupling agents.

The FTIR spectra of CDs from different silane coupling agents are as shown in Fig. 5d. The typical bands at 1030 and 1124 cm^{-1} originating from the stretching vibration of Si–O–Si, the absorption peak at 1657 cm^{-1} arises from –CONH– bond and the broad band within 3050–3650 cm^{-1} deriving from the stretching vibrations of O–H and N–H,[17] which represent CA all has reacted with different silane coupling agents.[20,29] The intensity of Si–O–Si, N–H and C=O peaks (relative to that of CONH) of CA-CDs are the highest, and the O–H band of CA-CDs are the widest, which further manifests that KH-792 has the highest degree of hydrolysis in the presence of CA and the reaction between CA and KH-792 are most complete, which leads to the highest QY of CA-CDs. Also, it has been proved that high N- and O-containing functional groups boost the QY of CDs.

The results of element analysis in Table S6† and the XPS spectra of CDs in Fig. S5† show that all CDs from different silane coupling agents are mainly composed of C, O and N with tiny amount of Si, and CA-CDs have the highest content of O. According to the element content analysis results of XPS (Table S7†), the element contents of CDs are of significant difference, because of the different contents of methoxy and amino groups on the surface of different silane coupling agents. These elements further influence the QY of CDs from different silane coupling agents, which is consistent with the results of CDs from different agents, which is consistent with the results of CDs from different carbon sources.

Fine scan XPS spectra of C 1s and O 1s for the CDs from different silane coupling agents are given in Fig. 5e, and the

Open Access Article. Published on 27 September 2022. Downloaded on 2/14/2026 12:02:08 AM.
This article is licensed under a Creative Commons Attribution-NonCommercial 3.0 Unported Licence.

Table 2 The amounts of various chemical bonds of CDs synthesized with different silane coupling agents in XPS spectra (carbon source is CA)

	C 1s			N 1s		
CDs	C–C/C=C/%	C–N/C–O/%	C=O/%	Pyridinic N/%	Amino N/%	Pyrrolic N/%
540-CDs	75.36	19.89	4.75	60.43	36.12	3.45
602-CDs	70.11	24.02	5.86	73.52	20.23	6.25
CA-CDs	64.03	29.53	6.44	63.82	27.37	8.81

percentage composition of each bond has quantificationally analysed as shown in Table 2. The C 1s spectrum indicates C mainly exists in forms of C–C/C=C, C–N/C–O and C=O. The N 1s spectra of CDs can validate the existence of pyridinic N, amino N and pyrrolic N.

With the peak intensity and the percentage composition of C=O and pyrrolic N separately on the surface of CDs gradually increased, the QY values of 540-, 602- and CA-CDs in Table S5† correspondingly increases. This proves that the content of C=O and pyrrolic N both have a positive effect on the QY of CDs from different silane coupling agents. The PY values of 540-, 602- and CA-CDs increase with the increasing amount of pyridinic N and the decreasing amount of amino N. This can indicate the high content of pyridinic N and low content of amino N contributes to the high PY of CDs from different silane coupling agents.

Optical properties. The UV-vis absorption spectra of the three kinds of CDs display two absorption peaks (Fig. S6†). The absorption peak at 360 nm is induced by the n–π* transition in the C=O bonds. The QY values of 602-CDs and CA-CDs are high and the corresponding absorption peaks at 360 nm are strong, which qualitatively shows the high content of C=O.[31] This is compatible with XPS results, indicating that high content of C=O is beneficial for the high QY of CDs.[27] It is can be seen that from the Fig. 6, 540-CDs with lowest QY value shows excitation wavelength-dependent property, whose fluorescent intensity is lower than the other two by comparison. On the contrary, the other two CDs with higher QY have the excitation wavelength-independent property. This result is consistent with the results of CDs from different carbon sources.

The fluorescence lifetimes of CDs from different silane coupling agents are presented in Fig. 6d and the corresponding parameters are shown in Table S8.† The decay curve of CA-CDs can be well fitted by a double exponential function and while the other two CDs can be fitted by a single exponential function. The slower the decay rate of lifetime, the higher the QY of CDs. Table S8† indicates the longer the lifetime of CDs, the higher the QY. It demonstrates the fluorescence of CDs from different silane coupling agents mainly derives from the surface state. Consequently, QY of CDs is mainly attributed to their surface structure.

Synergistic influence mechanism. In view of all above-mentioned factors, the possible structures of the three kinds of CDs are given in Fig. 7.

The difference in QY and PY of CDs from different silane coupling agents should not originate from the quantum size effect but surface state. Silane coupling agent contains different number of methoxy and amino groups, and different chain lengths, so the QY and PY values of corresponding synthesized CDs are different. KH-602 has one less methoxy group than KH-792, so the QY value of 602-CDs is slightly lower than that of CA-CDs, while KH-540 has a shorter chain length and one less amino group than KH-792, so the QY value of 540-CDs is much lower than that of CA-CDs, indicating amino groups have a significant effect on QY of CDs and methoxy group have little influence on QY of CDs. Specifically, the content of C=O and pyrrolic N both have a positive effect on the QY of CDs. Therefore, the organosilane functional groups including O- and N-containing functional groups make a significant contribution to high QY of CDs. It is because that on one hand, in the hydrothermal process, the amino group on the side chain of the silane coupling agent can react with the carboxyl group of CA to form an amide bond; on the other hand, each silane coupling agent contains two or three methoxy groups, after hydrolysis, they will form silanol groups which are highly reactive intermediates responsible for condensation with other silanes and hydroxyl groups from CA.[36]

Moreover, the PY values of 540-, 602- and CA-CDs were high and similar, from 46.33% to 58.53%, further verifying CDs with the crosslinked structure contributing to high PY, which is consistent with the results of CDs from different carbon

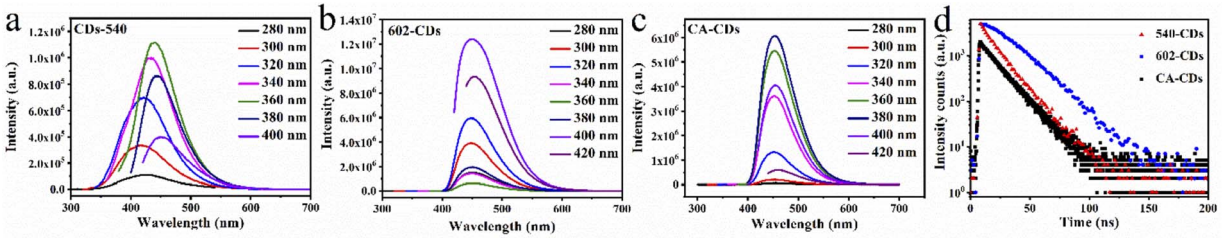

Fig. 6 (a–c) Fluorescence emission spectroscopy and (d) fluorescence decay curve of CDs synthesized with different silane coupling agents (carbon source is CA).

© 2022 The Author(s). Published by the Royal Society of Chemistry

Open Access Article. Published on 27 September 2022. Downloaded on 2/14/2026 12:02:08 AM.
This article is licensed under a Creative Commons Attribution-NonCommercial 3.0 Unported Licence.

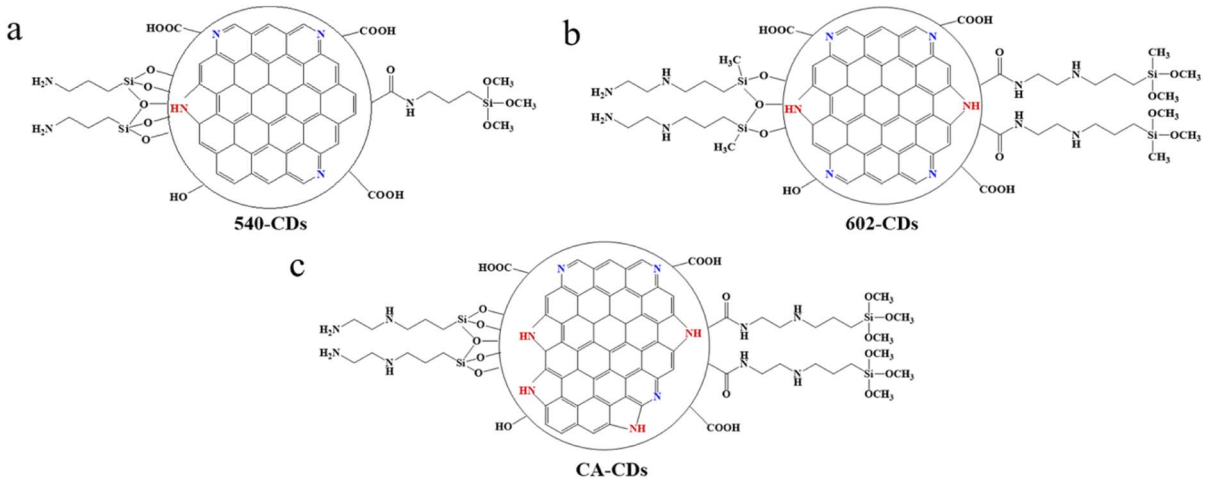

Fig. 7 Schematic structure of CDs synthesized with different silane coupling agents: (a) 540-CDs, (b) 602-CDs and (c) CA-CDs, carbon source is CA.

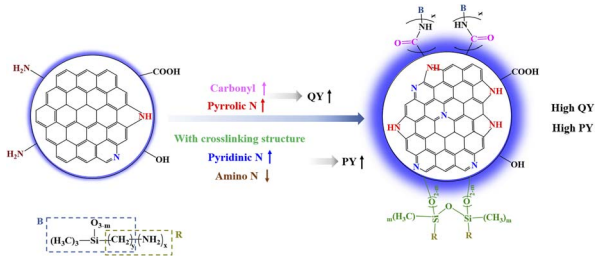

Fig. 8 Schematic of synergistic influence mechanism of O- and N-containing functional groups on CDs.

sources. Meanwhile, it is also found that high content of pyridinic N and low content of amino N favour for the high PY of CDs from different silane coupling agents.

In summary, the fluorescence of CDs from different silane coupling agents mainly depends on surface state luminescence not quantum size effect. The synergistic influence mechanism of O- and N- containing functional groups on CDs is presented, as shown in Fig. 8. The high content of C=O and pyrrolic N boost the QY enhancement of CDs. CDs with the property of excitation independence and long lifetime generally have high QY. CDs with the crosslinked structure generally have high PY, and high content of pyridinic N and the low content of amino N are in favor of CDs with high PY.

Conclusions

In conclusion, in order to explore the influence mechanism of O- and N-containing functional groups on CDs with high QY and PY, CDs were synthesized using different carbon sources and silane coupling agents with different content of O- and N-containing functional groups, respectively. Results indicated that the high contents of O- and N-containing functional groups (especially C=O bond and pyrrolic N) have a significant synergistic effect on the QY of CDs. CDs with the property of excitation independence and long lifetime generally have high QY. The highest QY of CDs is up to 97.32%. The PY value of CDs is closely related to the crosslink structure of CDs, and positively correlated with the pyridinic N content and negatively correlated with amino N. The PY of CDs is all above 46%. Therefore, the selection of raw materials rich in carboxyl groups and amino groups is conducive to the synthesis of high QY of CDs, and high content of pyrrolic N on CDs surface can enhance the QY. Furthermore, whether the reactants can undergo crosslink reaction also contributes to the PY values of CDs and high content of pyridinic N is favourable for preparing high PY of CDs. The above results provide theoretical guidance for synthesizing CDs with high QY on a large scale.

Author contributions

These authors contributed equally to the paper.

Conflicts of interest

The authors declare that they have no known competing financial interests or personal relationships that could have appeared to influence the work reported in this paper.

Acknowledgements

This work was funded by the Foundational Research Project of Shanxi Province (20210302123164, 20210302124604), Shanxi-Zheda Institute of Advanced Materials and Chemical Engineering (2021SX-TD012), National Natural Science Foundation of China (51972221), and Shanxi Scholarship Council of China (2020-051, HGKY2019027).

Notes and references

1 C. Wang, T. T. Hu, Z. Q. Wen, J. D. Zhou, X. J. Wang, Q. Wu and C. X. Wang, Concentration-dependent color tunability of nitrogen-doped carbon dots and their application for iron

Open Access Article. Published on 27 September 2022. Downloaded on 2/14/2026 12:02:08 AM. This article is licensed under a Creative Commons Attribution-NonCommercial 3.0 Unported Licence.

(III) detection and multicolor bioimaging, *J. Colloid Interface Sci.*, 2018, **521**, 33–41.

2 R. Atchudan, T. Edison, K. Aseer, S. Perumal, N. Karthik and Y. R. Lee, Highly fluorescent nitrogen-doped carbon dots derived from *Phyllanthus acidus* utilized as a fluorescent probe for label-free selective detection of Fe^{3+} ions, live cell imaging and fluorescent ink, *Biosens. Bioelectron.*, 2018, **99**, 303–311.

3 R. Atchudan, T. Edison, S. Perumal, N. Muthuchamy and Y. R. Lee, Hydrophilic nitrogen-doped carbon dots from biowaste using dwarf banana peel for environmental and biological applications, *Fuel*, 2020, **275**, 117821.

4 R. Atchudan, T. Edison, S. Perumal, R. Vinodh and Y. R. Lee, Betel-derived nitrogen-doped multicolor carbon dots for environmental and biological applications, *J. Mol. Liq.*, 2019, **296**, 111817.

5 R. Atchudan, T. Edison and Y. R. Lee, Nitrogen-doped carbon dots originating from unripe peach for fluorescent bioimaging and electrocatalytic oxygen reduction reaction, *J. Colloid Interface Sci.*, 2016, **482**, 8–18.

6 R. Atchudan, T. Edison, M. Sethuraman and Y. R. Lee, Efficient synthesis of highly fluorescent nitrogen-doped carbon dots for cell imaging using unripe fruit extract of Prunus mume, *Appl. Surf. Sci.*, 2016, **384**, 432–441.

7 M. Han, S. J. Zhu, S. Y. Lu, Y. B. Song, T. L. Feng, S. Y. Tao, J. J. Liu and B. Yang, Recent progress on the photocatalysis of carbon dots: classification, mechanism and applications, *Nano Today*, 2018, **19**, 201–218.

8 A. Tyagi, K. M. Tripathi, N. Singh, S. Choudhary and R. K. Gupta, Green synthesis of carbon quantum dots from lemon peel waste: applications in sensing and photocatalysis, *RSC Adv.*, 2016, **6**, 72423–72432.

9 X. L. Luo, W. G. Zhang, Y. Han, X. M. Chen, L. Zhu, W. Z. Tang, J. L. Wang, T. L. Yue and Z. H. Li, N, S co-doped carbon dots based fluorescent "on-off-on" sensor for determination of ascorbic acid in common fruits, *Food Chem.*, 2018, **258**, 214–221.

10 P. W. Gong, L. Sun, F. Wang, X. C. Liu, Z. Q. Yan, M. Z. Wang, L. Zhang, Z. Z. Tian, Z. Liu and J. M. You, Highly fluorescent N-doped carbon dots with two-photon emission for ultrasensitive detection of tumor marker and visual monitor anticancer drug loading and delivery, *Chem. Eng. J.*, 2019, **356**, 994–1002.

11 L. P. Yan, Y. Z. Yang, C. Q. Ma, X. G. Liu, H. Wang and B. S. Xu, Synthesis of carbon quantum dots by chemical vapor deposition approach for use in polymer solar cell as the electrode buffer layers, *Carbon*, 2016, **109**, 598–607.

12 Z. J. Zhou, P. F. Tian, X. Y. Liu, S. L. Mei, D. Zhou, D. Li, P. T. Jing, W. L. Zhang, R. Q. Guo, S. N. Qu and A. L. Rogach, Hydrogen peroxide-treated carbon dot phosphor with a bathochromic-shifted, aggregation-enhanced emission for light-emitting devices and visible light communication, *Adv. Sci.*, 2018, **5**, 1800369.

13 J. X. Zheng, Y. L. Wang, F. Zhang, Y. Z. Yang, X. G. Liu, K. P. Guo, H. Wang and B. S. Xu, Microwave-assisted hydrothermal synthesis of solid-state carbon dots with intensive emission for white light-emitting devices, *J. Mater. Chem. C*, 2017, **5**, 8105–8111.

14 Z. J. Zhu, R. Cheng, L. T. Ling, Q. Li and S. Chen, Rapid and large-scale production of multi-fluorescence carbon dots via magnetic hyperthermia method, *Angew. Chem., Int. Ed.*, 2020, **59**, 3099–3105.

15 Y. Q. Zhang, X. Y. Liu, Y. Fan, X. Y. Guo, L. Zhou, Y. Lv and J. Lin, One-step microwave synthesis of N-doped hydroxyl-functionalized carbon dots with ultra-high fluorescence quantum yields, *Nanoscale*, 2016, **8**, 15281–15287.

16 D. Qu, M. Zheng, L. G. Zhang, H. F. Zhao, Z. G. Xie, X. B. Jing, R. E. Haddad, H. Fan and Z. Sun, Formation mechanism and optimization of highly luminescent N-doped graphene quantum dots, *Sci. Rep.*, 2014, **4**, 5294.

17 S. S. Wu, W. Li, W. Zhou, Y. Zhan, C. F. Hu, J. L. Zhuang, H. R. Zhang, X. J. Zhang, B. F. Lei and Y. L. Liu, Large-scale one-step synthesis of carbon dots from yeast extract powder and construction of carbon dots/PVA fluorescent shape memory material, *Adv. Opt. Mater.*, 2018, **6**, 1701150.

18 Z. Y. Li, L. Wang, Y. Li, Y. Y. Feng and W. Feng, Frontiers in carbon dots: design, properties and applications, *Mater. Chem. Front.*, 2019, **3**, 2571–2601.

19 K. Yuan, X. H. Zhang, R. H. Qin, X. F. Ji, Y. H. Cheng, L. L. Li, X. J. Yang, Z. M. Lua and H. Liu, Surface state modulation of red emitting carbon dots for white light-emitting diodes, *J. Mater. Chem. C*, 2018, **6**, 12631.

20 Y. T. Xie, J. X. Zheng, Y. L. Wang, J. L. Wang, Y. Z. Yang, X. G. Liu and Y. K. Chen, One-step hydrothermal synthesis of fluorescence carbon quantum dots with high product yield and quantum yield, *Nanotechnology*, 2019, **30**, 085406.

21 A. N. Fletcher, Quinine sulfate as a fluorescence quantum yield standard, *Photochem. Photobiol.*, 1969, **9**, 439–444.

22 Q. Q. Shi, Y. H. Li, Y. Xu, Y. Wang, X. B. Yin, X. W. He and Y. K. Zhang, High-yield and high-solubility nitrogen-doped carbon dots: formation, fluorescence mechanism and imaging application, *RSC Adv.*, 2014, **4**, 1563–1566.

23 L. Wang, B. Q. Li, L. Li, F. Xu, Z. H. Xu, D. Q. Wei, Y. J. Feng, Y. M. Wang, D. C. Jia and Y. Zhou, Ultrahigh-yield synthesis of N-doped carbon nanodots that down-regulate ROS in zebrafish, *J. Mater. Chem. B*, 2017, **5**, 7848–7860.

24 Y. Q. Dong, H. C. Pang, H. B. Yang, C. X. Guo, J. W. Shao, Y. W. Chi, C. M. Li and Y. Ting, Carbon-based dots co-doped with nitrogen and sulfur for high quantum yield and excitation-independent emission, *Angew. Chem., Int. Ed.*, 2013, **52**, 1–6.

25 Y. F. Gao, H. L. Zhang, Y. Jiao, W. J. Lu, Y. Liu, H. Han, X. J. Gong, S. M. Shuang and C. Dong, Strategy for activating room-temperature phosphorescence of carbon dots in aqueous environments, *Chem. Mater.*, 2019, **31**, 7979–7986.

26 Y. F. Ding, J. X. Zheng, J. L. Wang, Y. Z. Yang and X. G. Liu, Direct blending of multicolor carbon quantum dots into fluorescent films for white light emitting diodes with an adjustable correlated color temperature, *J. Mater. Chem. C*, 2019, **7**, 1502.

27 S. J. Zhu, Y. B. Song, X. H. Zhao, J. R. Shao, J. H. Zhang and B. Yang, The photoluminescence mechanism in carbon dots

© 2022 The Author(s). Published by the Royal Society of Chemistry

Open Access Article. Published on 27 September 2022. Downloaded on 2/14/2026 12:02:08 AM.
This article is licensed under a Creative Commons Attribution-NonCommercial 3.0 Unported Licence.

(graphene quantum dots, carbon nanodots, and polymer dots): current state and future perspective, *Nano Res.*, 2015, **8**, 355–381.

28 C. J. Lin, Y. X. Zhuang, W. H. Li, T. L. Zhou and R. J. Xie, Blue, green, and red full-color ultralong afterglow in nitrogen-doped carbon dots, *Nanoscale*, 2018, **11**, 6584–6590.

29 Y. F. Wang, Z. M. Yin, Z. Xie, X. X. Zhao, C. J. Zhou, S. Y. Zhou and P. Chen, Polysiloxane functionalized carbon dots and their cross-linked flexible silicone rubbers for color conversion and encapsulation of white LEDs, *ACS Appl. Mater. Interfaces*, 2016, **8**, 9961–9968.

30 H. Ding, S. B. Yu, J. S. Wei and H. M. Xiong, Full-color light-emitting carbon dots with a surface-state-controlled luminescence mechanism, *ACS Nano*, 2015, **10**, 484–491.

31 B. Yuan, S. Y. Guan, X. M. Sun, X. M. Li, H. B. Zeng, Z. Xie, P. Chen and S. Y. Zhou, Highly efficient carbon dots with reversibly switchable green-red emission for trichromatic white light-emitting diodes, *ACS Appl. Mater. Interfaces*, 2018, **10**, 16005–16014.

32 H. F. Liu, Z. H. Li, Y. Q. Sun, X. Geng, Y. L. Hu, H. M. Meng, J. Ge and L. B. Qu, Synthesis of luminescent carbon dots with ultrahigh quantum yield and inherent folate receptor-positive cancer cell targetableity, *Sci. Rep.*, 2018, **8**, 1086.

33 F. Zhang, X. T. Feng, Y. Zhang, L. P. Yan, Y. Z. Yang and X. G. Liu, Photoluminescent carbon quantum dots as a directly film-forming phosphor towards white LEDs, *Nanoscale*, 2016, **8**, 8618–8632.

34 H. Ding, X. H. Li, X. B. Chen, J. S. Wei, X. B. Li and H. M. Xiong, Surface states of carbon dots and their influences on luminescence, *J. Appl. Phys.*, 2020, **127**, 231101.

35 Y. F. Wang, Master Degree, Shandong University, 2016.

36 Z. Xie, F. Wang and C. Y. Liu, Organic–inorganic hybrid functional carbon dot gel glasses, *Adv. Mater.*, 2012, **24**, 1716–1721.